Deletion of the von Hippel–Lindau gene in pancreatic β cells impairs glucose homeostasis in mice

James Cantley,[1] Colin Selman,[1] Deepa Shukla,[2] Andrey Y. Abramov,[3] Frauke Forstreuter,[2] Miguel A. Esteban,[2] Marc Claret,[1] Steven J. Lingard,[1] Melanie Clements,[1] Sarah K. Harten,[2] Henry Asare-Anane,[4] Rachel L. Batterham,[1] Pedro L. Herrera,[5] Shanta J. Persaud,[4] Michael R. Duchen,[3] Patrick H. Maxwell,[2] and Dominic J. Withers[1]

[1]Centre for Diabetes and Endocrinology and [2]Centre for Cell Signalling and Molecular Genetics, Faculty of Medicine, Rayne Institute, and [3]Department of Physiology and Mitochondrial Biology Group, University College London, London, United Kingdom. [4]Beta Cell Development and Function Group, Division of Reproductive Health, Endocrinology and Development, King's College London, London, United Kingdom. [5]Department of Genetic Medicine and Development, Faculty of Medicine, University of Geneva, Geneva, Switzerland.

Defective insulin secretion in response to glucose is an important component of the β cell dysfunction seen in type 2 diabetes. As mitochondrial oxidative phosphorylation plays a key role in glucose-stimulated insulin secretion (GSIS), oxygen-sensing pathways may modulate insulin release. The von Hippel–Lindau (VHL) protein controls the degradation of hypoxia-inducible factor (HIF) to coordinate cellular and organismal responses to altered oxygenation. To determine the role of this pathway in controlling glucose-stimulated insulin release from pancreatic β cells, we generated mice lacking *Vhl* in pancreatic β cells (β*VhlKO* mice) and mice lacking *Vhl* in the pancreas (*PVhlKO* mice). Both mouse strains developed glucose intolerance with impaired insulin secretion. Furthermore, deletion of *Vhl* in β cells or the pancreas altered expression of genes involved in β cell function, including those involved in glucose transport and glycolysis, and isolated β*VhlKO* and *PVhlKO* islets displayed impaired glucose uptake and defective glucose metabolism. The abnormal glucose homeostasis was dependent on upregulation of Hif-1α expression, and deletion of *Hif1a* in Vhl-deficient β cells restored GSIS. Consistent with this, expression of activated Hif-1α in a mouse β cell line impaired GSIS. These data suggest that VHL/HIF oxygen-sensing mechanisms play a critical role in glucose homeostasis and that activation of this pathway in response to decreased islet oxygenation may contribute to β cell dysfunction.

Introduction

Blood glucose levels are normally tightly controlled by the regulation of insulin release from the pancreatic β cells. Glucose-stimulated insulin secretion (GSIS) is a complex metabolic process involving the uptake and phosphorylation of glucose via GLUT2 transporters and glucokinase (Gck), respectively, metabolism of glucose-6-phosphate via the glycolytic pathway, and subsequent activation of mitochondrial metabolism to produce coupling factors such as ATP (1). A rise in the cytoplasmic ATP/ADP ratio leads to closure of K_{ATP} channels, depolarization of the plasma membrane, opening of voltage-sensitive Ca^{2+} channels, and activation of Ca^{2+}-dependent exocytotic mechanisms, resulting in insulin secretion (1). This metabolic sensing mechanism requires molecular oxygen for the quantitative generation of ATP from glucose. Understanding the complex physiology of this mechanism may give insights into both the pathogenesis and treatment of the β cell dysfunction seen in type 2 diabetes.

Hypoxia-inducible factor (HIF) is a transcription control complex containing a constitutive β subunit and regulatory α subunit, which acts as a master regulator of the responses to altered cellular and tissue oxygen concentration (2). In the presence of oxygen, HIF-α subunits are hydroxylated, enabling capture by the von Hippel–Lindau (VHL) tumor suppressor gene product, which is the substrate recognition component of an ubiquitin E3 ligase complex (3, 4). At low oxygen concentrations, HIF-α is stabilized and active. In the absence of VHL, HIF is constitutively active. Key processes regulated by HIF include erythropoiesis, angiogenesis, and cellular energy metabolism, thereby adapting the organism, tissue, and cell to hypoxia (4). HIF is responsive within the range of oxygen tensions encountered in normal tissues and is increasingly recognized as an important physiological regulator rather than a simple stress response mechanism, playing roles, for example, in innate immunity (5), neutrophil survival (6), muscle performance (7), and skin oxygen sensing (8).

HIF upregulates expression of the high-affinity glucose transporter GLUT1 and glycolytic enzymes and decreases mitochondrial oxygen consumption in a range of cell types (4). Since glucose uptake, glycolysis, and mitochondrial respiration are key steps in β cell glucose sensing, activation of the HIF pathway has the potential to provide a major input modulating GSIS. This could potentially be important in a wide range of disease states in which oxygen delivery is altered, including obstructive sleep apnea and acute and chronic respiratory disease, or when islet oxygenation is directly compromised, such as

Figure 1
Deletion of *Vhl* in β cells or the pancreas impairs glucose homeostasis in mice. (**A**) Recombination of the *Vhl* allele was assayed by PCR in islets, cerebral cortex (cortex), and hypothalami (hyp) from WT and KO mice for β*VhlKO* and *PVhlKO* mice. Positive and negative PCR controls for deletion were performed using DNA from *Vhl*-null cells, *Vhl* control (cont) cells, WT cells, and without addition of DNA. Arrows indicate the deleted allele. (**B** and **C**) Hif-1α staining using chromogenic detection (left and middle panels) in islets from control, β*VhlKO*, and *PVhlKO* mice and combined chromogenic/immunofluorescence staining (right panels) co-localizing Hif-1α and insulin in islets from β*VhlKO* and *PVhlKO* mice. (**D** and **E**) Fed blood glucose levels in 12-week-old female control, β*VhlKO*, and *PVhlKO* mice. $n = 8$. (**F** and **G**) Blood glucose after an intraperitoneal injection (2 g/kg body weight) of glucose in 12-week-old female control, β*VhlKO*, and *PVhlKO* mice. $n = 8$ for null alleles; $n = 24$ for control animals. (**H** and **I**) Fed plasma insulin levels in 12-week-old female control, β*VhlKO*, and *PVhlKO* mice. $n = 8$. *$P < 0.05$, **$P < 0.01$, ***$P < 0.001$ compared with control.

in islet transplantation. VHL disease is associated with pancreatic tumors believed to be of endocrine origin, also indicating a potential role for this pathway in islet endocrine cell growth and function. Furthermore, small-molecule HIF activators are currently under evaluation for the treatment of anemia, and understanding the potential effects of pharmacological manipulation of this pathway on pancreatic islet function is also of clinical interest.

Therefore, to determine the effect of activating HIF, we investigated the effect of deleting the *Vhl* gene, specifically in β cells or the pancreas in mice. After we initiated these studies, it was reported that islets of patients with type 2 diabetes show reduced expression of the HIF-α dimerization component aryl hydrocarbon receptor nuclear translocator/*HIF1b* (*ARNT/HIF1B*) and that knockdown of *Arnt/Hif1b*

in β cells or mice impaired GSIS (9). In light of these studies, and assuming a monotonic relationship between GSIS and HIF activation, it was reasonable to predict that HIF activation would have the opposite effect of deletion of *Arnt/Hif1b* and therefore enhance GSIS. Our genetic experiments showed that Hif activation in mice results in profound disruption of β cell function and, in contrast, that β cell deletion of *Hif1a* does not impair glucose homeostasis.

Results

Deletion of Vhl in β cells or in the pancreas impairs glucose homeostasis in mice. Initially, we crossed mice expressing Cre under control of the rat insulin II promoter (*RIPCre* mice; ref. 10) and mice with a floxed allele of *Vhl* (11) to generate mice lacking *Vhl* in pancreatic
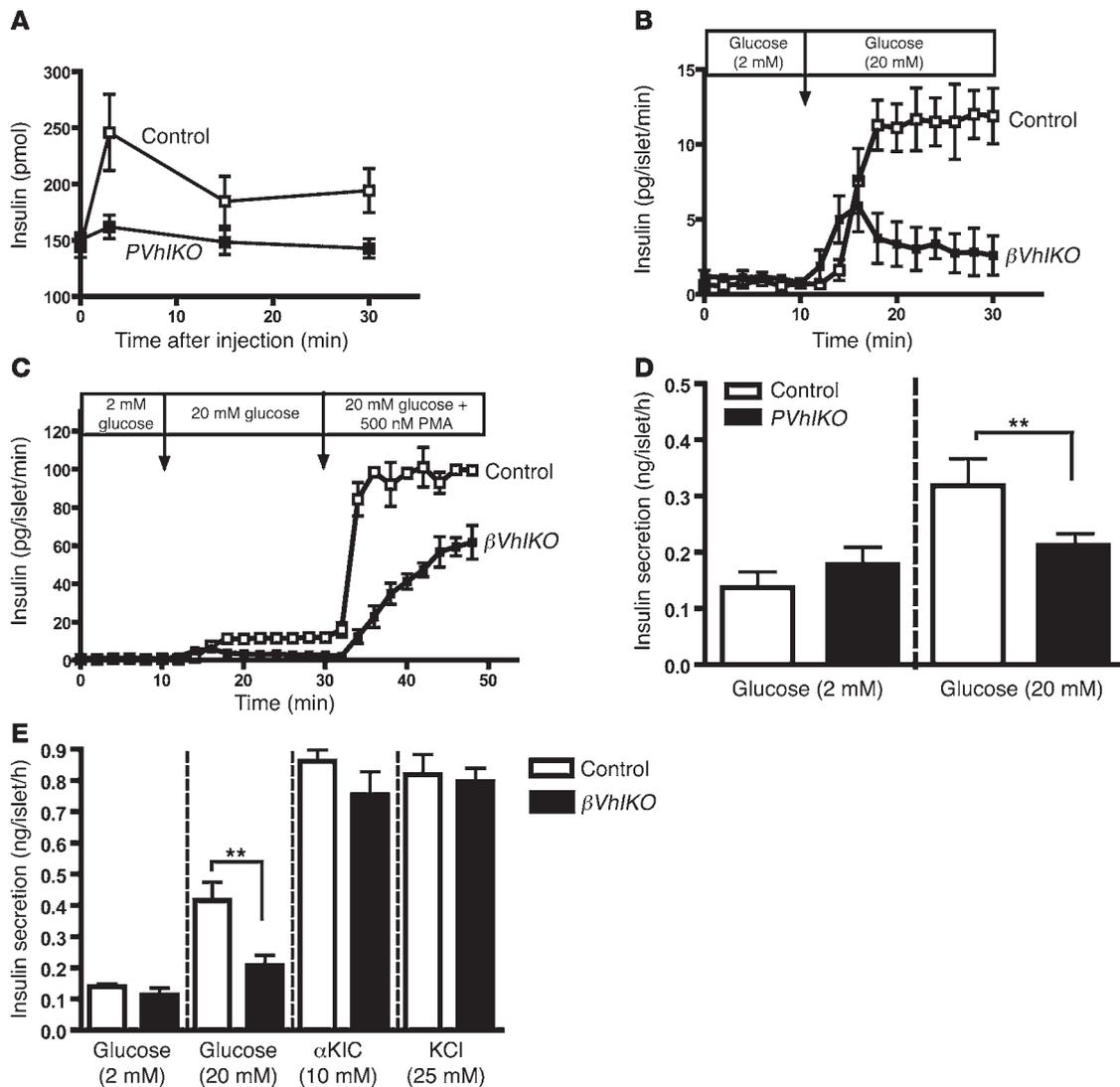
Figure 2

Defective GSIS in mice lacking *Vhl* in β cells or the pancreas. (**A**) Plasma insulin levels before and after an intraperitoneal injection of glucose (3 g/kg body weight) in 12-week-old female control (open squares) and *PVhlKO* (filled squares) mice. *n* = 7–9 per genotype. (**B** and **C**) Insulin secretion from isolated control (open squares) and β*VhlKO* islets (closed squares) in response to perifusion with 2 and 20 mmol/l glucose and 500 nmol/l phorbol ester (PMA). *n* = 3. (**D**) Insulin secretion from isolated control and *PVhlKO* islets in static cultures in response to 2 and 20 mmol/l glucose. *n* = 5. (**E**) Insulin secretion from isolated control and β*VhlKO* islets in static cultures in response to 2 and 20 mmol/l glucose, 10 mmol/l α-ketoisocaproic acid (αKIC), and 25 mmol/l potassium chloride (KCl). *n* = 8. **P < 0.01.

β cells (β*VhlKO* mice) and in a small population of hypothalamic neurons (12). β*VhlKO* mice were viable and born with expected Mendelian ratios (data not shown). The *Vhl* allele was deleted in islets and hypothalami from β*VhlKO* mice (Figure 1A), and Hif-1α stabilization and expression was induced in more than 95% of β cells of β*VhlKO* mice, consistent with *Vhl* deletion (Figure 1B and Supplemental Figure 1A; supplemental material available online with this article; doi:10.1172/JCI26934DS1). However, β*VhlKO* mice were proportionate dwarfs with reduced pituitary growth hormone (GH) levels (Supplemental Figure 1, B and C), while relative food intake and fat mass were normal in these animals (Supplemental Figure 1, D and E). These findings suggest that Vhl acts in *RIPCre* hypothalamic neurons to regulate Gh secretion. This endocrine phenotype may have had an impact on subse-

quent studies of glucose homeostasis in β*VhlKO* mice. Therefore, to test the possibility that potential β cell phenotypes in β*VhlKO* mice resulted wholly or partly from hypothalamic deletion of *Vhl*, we used mice expressing Cre under control of the mouse pancreatic and duodenal homeobox 1 promoter (*PdxCre* mice) to generate *PVhlKO* mice, which lacked *Vhl* only in the pancreas (13, 14). *PVhlKO* mice were born with the expected Mendelian frequency and, in contrast to β*VhlKO* mice, displayed normal body weight (Supplemental Figure 1F). Recombination of the *Vhl* allele was observed in *PVhlKO* islets but not in hypothalami (Figure 1A). Stabilization and expression of Hif-1α was induced in the pancreas of *PVhlKO* mice (Figure 1C) with greater than 70% of β cells expressing Hif-1α and a 70% reduction in *Vhl* mRNA (Supplemental Figure 1, G and H). We did not detect Hif-2α in the pancreas
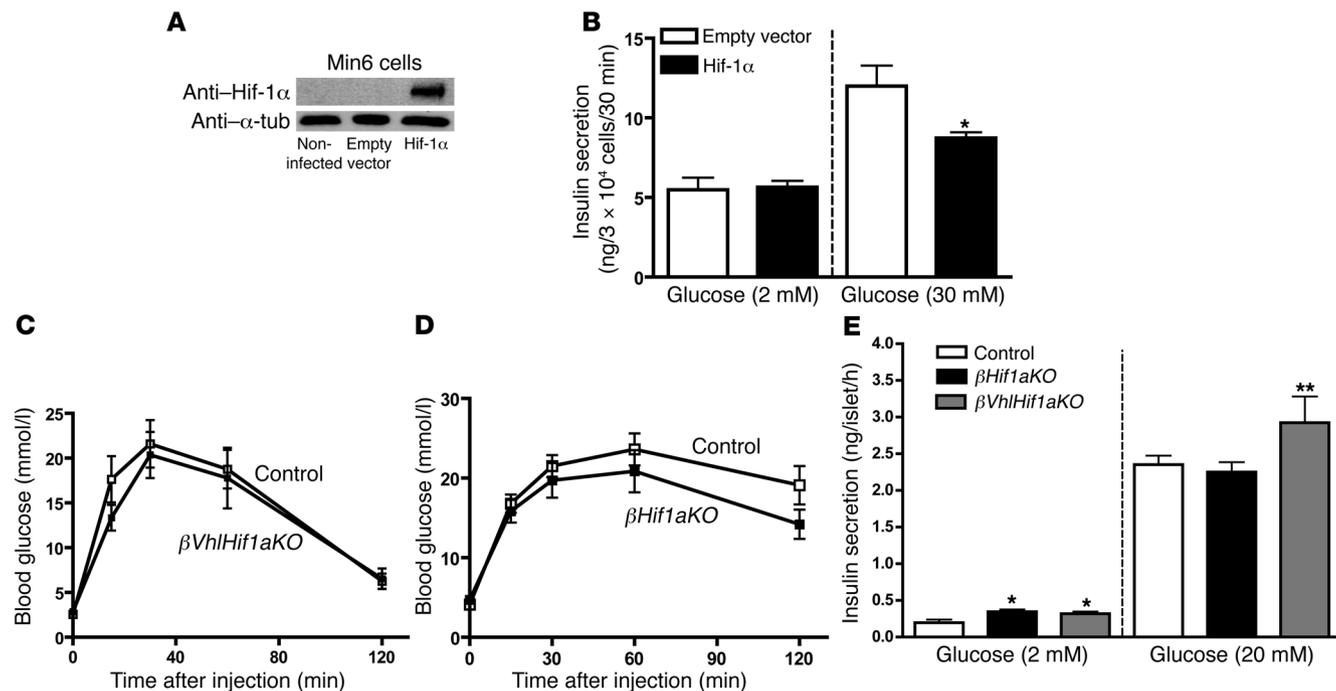
Figure 3
Dependence of abnormal glucose homeostasis on upregulation of Hif-1α and phenotype of βHif1aKO mice. (**A**) Western blot for Hif-1α and tubulin loading control in Min6 cells transfected with activated Hif-1α mutant. α-tubulin was resolved on a 10% gel, and Hif-1α was analyzed on a separate 6% gel after equal amounts of the same cell lysate were loaded. Blots are typical of 2 independent experiments. (**B**) Insulin secretion from Min6 cells transfected with activated Hif-1α mutant or empty vector in response to 2 and 30 mmol/l glucose. n = 5. (**C**) Blood glucose after an intraperitoneal injection (2 g/kg body weight) of glucose in 4- to 6-month-old male control (open squares) and βVhlHif1aKO (filled squares) mice. n = 8. (**D**) Blood glucose after an intraperitoneal injection (2 g/kg body weight) of glucose in 4- to 6-month-old male control (open squares) and βHif1aKO (filled squares) mice. n = 8. (**E**) Insulin secretion from isolated control, βHif1aKO, and βVhlHif1aKO islets from 4- to 6-month-old male mice in static cultures in response to 2 and 20 mmol/l glucose. n = 8. *P < 0.05, **P < 0.01 compared with control.

of βVhlKO or PVhlKO mice, and pancreatic weight was normal in PVhlKO mice with no clinical evidence of exocrine dysfunction in these animals (data not shown).

Generation of βVhlKO and PVhlKO mice permitted examination of the role of Vhl in glucose homeostasis in vivo. Twelve-week-old female βVhlKO and PVhlKO mice displayed significantly elevated fed glucose levels and impaired glucose tolerance (Figure 1, D–G). Glucose intolerance was also seen in 12-week-old male βVhlKO and PVhlKO mice (Supplemental Figure 2, A and B). Fed insulin levels were reduced in both βVhlKO and PVhlKO mice (Figure 1, H and I), fasting insulin levels in PVhlKO mice were similar to those seen in control animals, and βVhlKO mice displayed a mild fasting hypo-insulinemia compared with control mice (Supplemental Figure 2, C and D). Insulin tolerance tests in PVhlKO mice demonstrated no impairment of insulin sensitivity (data not shown). The similarity of the glucose homeostasis phenotypes in both βVhlKO and PVhlKO mice indicated that this was not due to the hypothalamic deletion of Vhl seen in the βVhlKO animals.

Deletion of Vhl in β cells or in the pancreas does not alter β cell mass, proliferation, or survival or cause pancreatic tumors. The VHL/HIF pathway has been implicated in both growth factor–mediated cell proliferation and cell survival. Therefore, we undertook islet morphometric analysis in βVhlKO and PVhlKO mice to exclude reduction of β cell mass as the cause for the impaired glucose homeostasis. Absolute β cell mass was reduced in βVhlKO animals, but when expressed as a percentage of body mass was equivalent to that in control mice

(Supplemental Figure 3, A and B). β cell area in βVhlKO mice was equivalent to that seen in control animals (Supplemental Figure 3C). Likewise, we detected no significant difference in β cell mass (either expressed as an absolute value or as a function of body weight) or β cell area in PVhlKO mice compared with control animals (Supplemental Figure 3, D–F). Consistent with these findings, there were no alterations in β cell apoptosis or proliferation rates in both strains (Supplemental Figure 3, G and H). In both mouse lines, organization of α and β cells was preserved, but in βVhlKO mice occasional α cells were scattered among the β cells (Supplemental Figure 4, A and B). Taken together, these findings imply that the in vivo defects in glucose handling were not the result of ablation of β cells. We did detect alteration in the vascularization of the pancreas in βVhlKO and PVhlKO mice by staining for Cd31, although expression of this vascular marker as determined by RT-PCR was not increased in βVhlKO and PVhlKO islets compared with those of controls (Supplemental Figure 4, C–E). Interestingly, however, and consistent with the normal cell proliferation and survival parameters, we did not detect tumors or cyst formation in the pancreases of βVhlKO or PVhlKO mice up to 12 months old (data not shown), suggesting that these pathologies arise from cell types other than those in which we deleted Vhl (i.e., β cells or Pdx1-expressing cells) or involve additional events such as expression of Hif-2α (15).

Deletion of Vhl impairs GSIS in vivo and in vitro. The absence of changes in β cell mass in the islets of βVhlKO or PVhlKO mice suggested that functional defects in β cells underlie the alterations in
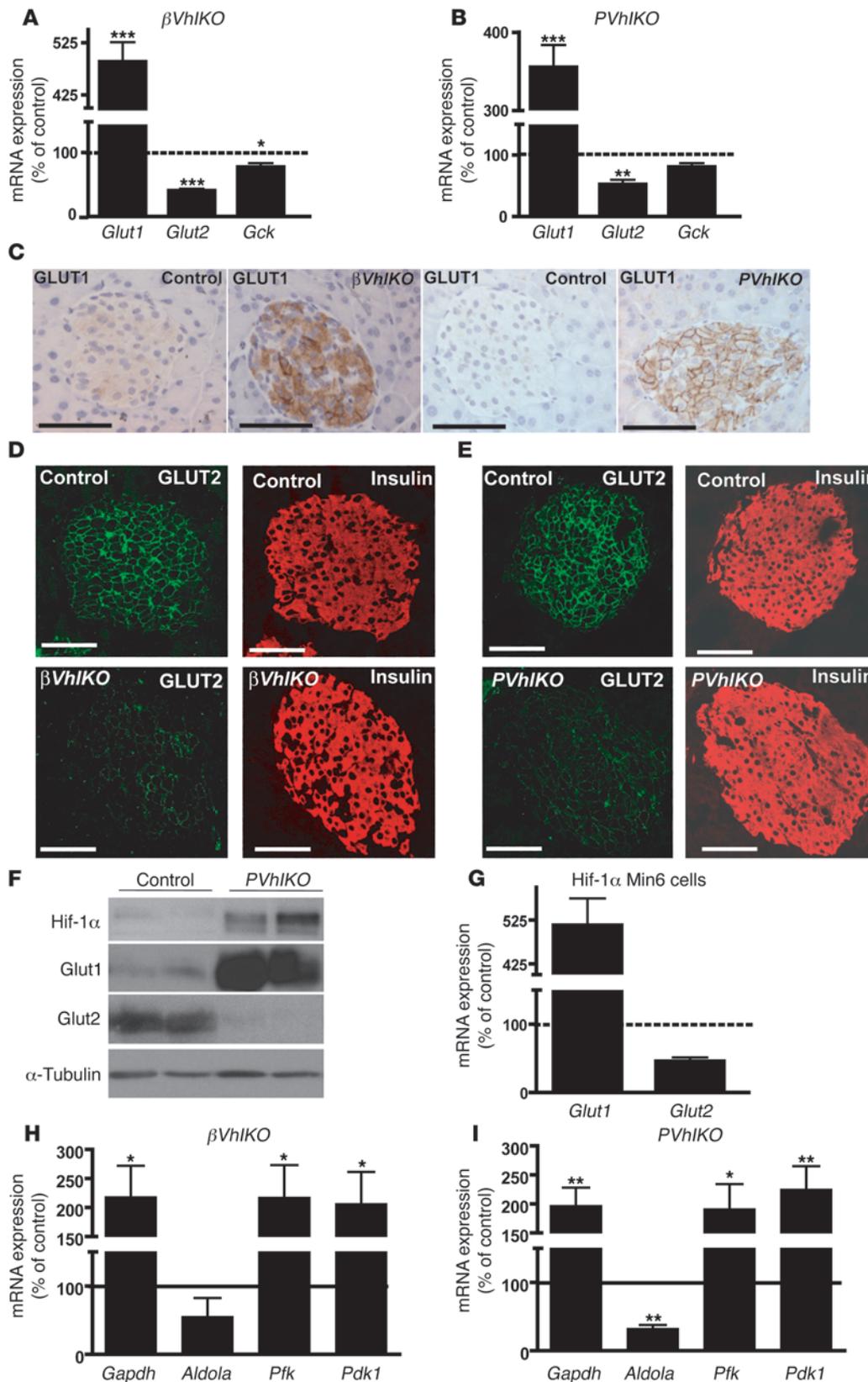
Figure 4
Abnormal expression of glucose-sensing apparatus and glycolytic genes in β*VhlKO* and *PVhlKO* mice. (**A** and **B**) Expression of *Glut1*, *Glut2*, and *Gck* mRNA in β*VhlKO* and *PVhlKO* islets relative to control islets. $n = 5$. (**C**) Glut1 immunostaining in control, β*VhlKO*, and *PVhlKO* islets. Representative images are shown. Scale bars: 150 μm. (**D** and **E**) Glut2 (green) and insulin (red) staining in control, β*VhlKO*, and *PVhlKO* islets. Representative images are shown. Scale bars: 100 μm. (**F**) Western blotting for Hif-1α, Glut1, Glut2, and α-tubulin (loading control) in islets isolated from *PVhlKO* mice. Glut1, Glut2, and α-tubulin were resolved on a 10% gel, and blots were probed and stripped for each of the 3 antibodies. Hif-1α was analyzed on a separate 6% gel with an equal amount of the same cell lysate loaded. Representative blots are shown and are typical of 2 independent experiments. (**G**) Expression of *Glut1* and *Glut2* mRNA in Min6 cells transfected with activated *HIF1α* mutant relative to empty vector–transfected control cells. $n = 3$. (**H** and **I**) Expression of *Gapdh*, *Aldola*, *Pfk*, and *Pdk1* mRNA in isolated β*VhlKO* and *PVhlKO* islets relative to control islets. $n = 5$. *$P < 0.05$, **$P < 0.01$, ***$P < 0.001$ compared with control.
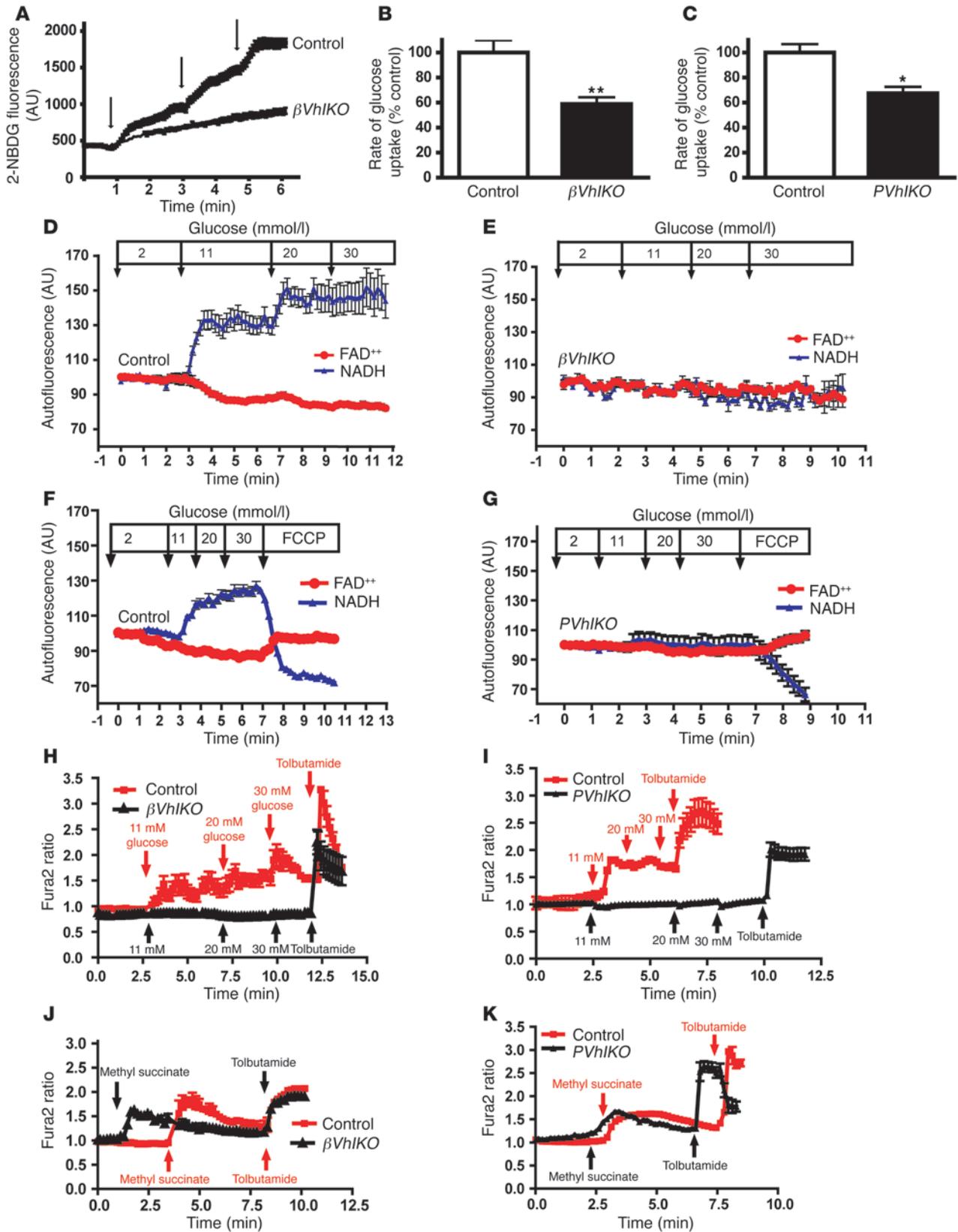
Figure 5

Glucose uptake and metabolism is impaired in β cells lacking *Vhl*, but mitochondrial function is preserved. (**A**) Continuous monitoring of 2-NBDG uptake (18 nmol/l added at the time points indicated by vertical arrows) into control and β*VhlKO* β cells incubated in 2.5 mmol/l D-glucose. (**B** and **C**) Rate of uptake of 2-NBDG into β cells from control, β*VhlKO*, and *PVhlKO* mice. *n* = 8 groups of β cells from 3 animals of each genotype. *P < 0.05, **P < 0.01 compared with control. (**D–G**) NADH and FAD++ autofluorescence was monitored by confocal microscopy for control (**D** and **F**), β*VhlKO* (**E**), and *PVhlKO* (**G**) β cells at the indicated glucose concentrations. Results are expressed as a percentage of basal values ± SEM for 8 groups of β cells from 3 animals of each genotype. (**H** and **I**) Ca²⁺ signals in response to indicated glucose concentrations and tolbutamide (200 μmol/l) in control, β*VhlKO*, and *PVhlKO* β cells. Recordings were made from 50 cells of each genotype from 2 animals of each genotype. (**J** and **K**) Ca²⁺ signals in response to methyl succinate (10 mmol/l) in control, β*VhlKO*, and *PVhlKO* β cells. Recordings were made from 50 cells of each genotype from 2 animals of each genotype.

glucose homeostasis. Consistent with this idea, in vivo GSIS was severely blunted in *PVhlKO* mice (Figure 2A). To define the nature of the defects in GSIS seen with the deletion of *Vhl*, we undertook further in vitro analysis of β cell function using isolated islets and β cells. In perifusion studies, insulin release was equivalent in isolated control and β*VhlKO* islets under basal conditions (2 mmol/l glucose; Figure 2B). As the perifusate glucose concentration was increased to 20 mmol/l, peak and sustained GSIS were markedly impaired in β*VhlKO* islets (Figure 2B). When the same islets were challenged with 20 mmol/l glucose and 500 nmol/l phorbol ester to induce potentiated insulin release, β*VhlKO* islets had a response that reached 60% of control islets, suggesting significant preservation of the response to a non-glucose potentiator of GSIS (Figure 2C). In static incubation experiments, GSIS was also markedly impaired in *PVhlKO* islets (Figure 2D). To further probe the site of the defective GSIS we used the non-glucose secretagogues α-ketoisocaproic acid (which is exclusively metabolized in mitochondria) and potassium chloride (which depolarizes β cell membranes independently of glucose metabolism). Stimulated insulin secretion in β*VhlKO* islets was normal with both of these agents, while GSIS was again impaired, suggesting that the defect is proximal to mitochondrial metabolism (Figure 2E).

Increased expression of constitutively activated HIF-1α in β cells impairs GSIS. We next examined whether the defects in GSIS could result from increased activation of HIF-1α using a mouse β cell line. Elevated expression of HIF-1α was achieved in Min6 cells transduced with a retrovirus expressing a constitutively active HIF-1α (Figure 3A). Examination of these cells revealed impaired insulin release in response to glucose, indicating that activation of HIF-1α perturbs GSIS (Figure 3B).

*Rescue of defective glucose homeostasis in β*VhlKO* mice by concomitant deletion of Hif1a and lack of glucose homeostasis phenotype in β*Hif1aKO* mice.* To test genetically in vivo the role of Hif-1α in mediating the perturbation in glucose homeostasis following *Vhl* deletion, we generated mice lacking both *Vhl* and *Hif1a* in pancreatic β cells (β*VhlHif1aKO* mice) using a mouse with a floxed allele of *Hif1a*. These mice had normal fasted and fed blood glucose levels (Supplemental Figure 4, F and G) and normal glucose tolerance at 4–6 months of age (Figure 3C). Furthermore the dwarf phenotype seen in β*VhlKO* mice was reversed in these animals (Supplemental Figure 4H).

The generation of β*Hif1aKO* mice, which lack *Hif1α* in RIPCre-expressing cells as part of the genetic crosses used to breed β*VhlHif1aKO* mice, also permitted us to analyze the impact of reduced Hif-1α activity upon glucose homeostasis. These animals, which had normal body weight (Supplemental Figure 4I), displayed normal glucose handling on glucose tolerance testing at both 12 weeks and 4–6 months of age (Figure 3D and Supplemental Figure 4J). Studies in isolated islets from these mice revealed a slight but significant increase in insulin release under basal (2 mmol/l) glucose conditions, but no difference in GSIS compared with control mice (Figure 3E). Furthermore, when we examined GSIS in islets from β*VhlHif1aKO* mice, this was slightly enhanced compared with that seen in control animals (Figure 3E). Together, these findings suggest that Hif-1α may have a mild restraining effect upon β cell function and that the abnormal GSIS seen in β*VhlKO* mice is dependent upon upregulation of Hif-1α.

These results indicate that appropriate expression of Hif-1α is required for normal β cell function, and for GSIS in particular. The rescue of the phenotype of β*VhlKO* mice by concomitant deletion of *Hif1a*, the defective GSIS in cells expressing constitutively active HIF-1α, and the concordant phenotype seen in *PVhlKO* mice suggest that this abnormality is not the result of other features that may be present in the β*VhlKO* mice due to the hypothalamic deletion.

Alteration in expression of key components of the glucose-sensing apparatus and glycolytic pathway in islets lacking Vhl. The profound defects in GSIS in the absence of abnormalities in β cell mass and the preserved insulin release in response to α-ketoisocaproic acid suggested that β cells lacking *Vhl* had abnormalities in glucose-sensing or in the proximal elements of glucose metabolism. We therefore examined expression of components of the glucose-sensing and glycolytic apparatus, which are known targets of the VHL/HIF pathway. In both β*VhlKO* and *PVhlKO* islets, there was a significant reduction of *Glut2* mRNA expression and a concomitant induction in *Glut1* mRNA expression with parallel changes in Glut2 and Glut1 production in pancreatic sections and in isolated islets (Figure 4, A–F). In particular, there was a striking loss of cell membrane Glut2 immunofluorescence and protein production in β*VhlKO* and *PVhlKO* islets (Figure 4, D–F). Expression of *Gck* mRNA was also reduced in islets of both genotypes (Figure 4, A and B). *Glut1* expression was increased and *Glut2* expression was reduced in Min6 cells expressing constitutively active HIF-1α or exposed either to hypoxia or the HIF activator dimethyloxalylglycine (16) (Figure 4G and Supplemental Figure 5, A and B), supporting the conclusion that the observed expression changes in β*VhlKO* and *PVhlKO* islets are mediated by increased Hif-1α activity.

Analysis of the expression of a panel of glycolytic genes revealed that expression of pyruvate dehydrogenase kinase 1 (*Pdk1*), phosphofructokinase (*Pfk*), and *Gapdh* was increased in islets isolated from β*VhlKO* and *PVhlKO* mice, while aldolase expression was reduced (Figure 4, H and I). Increased *Pdk1* expression inhibits pyruvate dehydrogenase activity and restricts the entry of pyruvate to mitochondrial oxidative pathways, while reduced aldolase expression further contributes to reducing flux through glycolysis.

We next examined the expression of key β cell transcription factors. In both β*VhlKO* and *PVhlKO* islets, there was a significant reduction in the expression of *Nkx6.1*, a homeodomain transcription factor that regulates GSIS in β cells (17) (mRNA expression as a percentage of control: β*VhlKO*, 51.5% ± 11.5% vs. control, 100.0% ± 10.1%, *P* < 0.01, *n* = 6; *PVhlKO*, 56.6% ± 3.4% vs. control, 100.0% ± 13.8%, *P* < 0.05, *n* = 5). In contrast, the expression of hepa-

tocyte nuclear factor 1a (*Hnf1a*), *Hnf3b*, *Hnf4a*, and *NeuroD* was unaltered (data not shown). The glycoprotein E-cadherin (*Ecad*) has been implicated in β cell function (18), and we have recently demonstrated that the VHL/HIF pathway suppresses its expression in renal cancer cells (19). In both β*VhlKO* and *PVhlKO* islets, expression of *Ecad* was reduced (mRNA expression as a percentage of control: β*VhlKO*, 46.6% ± 5.3% vs. control, 100% ± 10%, $P < 0.01$, $n = 6$; *PVhlKO*, 39.7% ± 2.0% vs. control, 100% ± 10.7%, $P < 0.01$, $n = 5$).

Islets lacking Vhl have impaired glucose uptake and metabolism. The net effect of the expression changes in glucose-sensing and glycolytic genes might be expected to reduce coupling of glucose uptake and glycolysis to mitochondrial ATP production and insulin secretion. Therefore, we undertook further functional analysis in islets isolated from β*VhlKO* and *PVhlKO* mice, initially studying glucose uptake by isolated β cells. Control β cells incubated in 2.5 mmol/l glucose rapidly took up 2-(*N*-[7-nitrobenz-2-oxa-1,3-diazol-4-yl]amino)-2-deoxy-D-glucose (2-NBDG), a fluorescent D-glucose derivative (20) (Figure 5A). In contrast, both total steady-state fluorescence and the rate of 2-NBDG uptake were significantly reduced in β*VhlKO* and *PVhlKO* islets (Figure 5, A–C, and data not shown).

Next we monitored the increase in metabolic flux as glucose is metabolized by β cells, by measuring cellular NADH and flavin adenine dinucleotide (FAD++) levels using autofluorescence (21). In response to increasing glucose concentrations, control β cells exhibited a robust increase in NADH and a concomitant fall in FAD++ fluorescence (Figure 5, D and F). In contrast, these responses were essentially absent in β*VhlKO* and *PVhlKO* β cells, indicating altered mitochondrial metabolism in response to glucose (Figure 5, E and G). To probe the site of this defect, we monitored Ca²⁺ fluxes in Fura-2AM–loaded β cells from β*VhlKO* and *PVhlKO* mice in response to glucose, methyl-succinate (which enters the mitochondrial respiratory chain at complex II) and the K_ATP channel blocker tolbutamide. Glucose-stimulated Ca²⁺ mobilization was markedly attenuated in β*VhlKO* and *PVhlKO* β cells compared with controls (Figure 5, H and I). In contrast, responses to methyl-succinate and tolbutamide were preserved in β*VhlKO* and *PVhlKO* β cells (Figure 5, J and K), which, in combination with the normal secretory response to α-ketoisocaproic acid (Figure 2E), places the defect in GSIS between the glucose uptake machinery and mitochondrial metabolism. Taken together with the abnormalities in the proximal components of the glucose-sensing apparatus, these findings demonstrate that the VHL/HIF pathway is critical in regulating mammalian pancreatic β cell function.

Discussion

Pancreatic β cells have high rates of aerobic metabolism compared with other cell types, and islet oxygenation is markedly higher than in the exocrine pancreas or other tissues (22). In the current studies, we investigated whether inactivation of *Vhl* in β cells and concomitant Hif activation alters glucose sensing. Although available transgenic lines are effective at β cell deletion, they are not completely selective (12, 13). We therefore used 2 inactivation strategies, both of which inactivated *Vhl* in β cells. The concordant defects in GSIS that we observed in β*VhlKO* and *PVhlKO* mice, combined with our analyses of isolated islets, imply that loss of *Vhl* in the β cell results in a profound defect in GSIS.

The most extensively studied function of VHL is its role in the destruction of HIF-1α and HIF-2α in the presence of oxygen (3). VHL also interacts with a number of other proteins and influences diverse intracellular pathways (reviewed in ref. 23). Proteins that have been reported to interact with VHL in other cell types, and which

could alter glucose uptake and GSIS in β cells, include PKC-λ/ι and -δ (24, 25) and Sp1 (26). To determine whether the effects of *Vhl* loss of function were mediated by Hif-1α, we therefore generated β*VhlHif1aKO* mice. Our finding of normal glucose homeostasis and body weight in β*VhlHif1aKO* mice suggests that the alteration in both these parameters caused by deletion of *Vhl* is mediated via activation of Hif-1α. This experiment does not formally exclude the possibility that hypothalamic deletion of *Hif1a* in β*VhlHif1aKO* mice contributes to the correction of glucose homeostasis. Nevertheless, our data on β cells expressing a constitutively activated HIF-1α show that HIF-1α activation is sufficient to have major effects on GSIS and gene expression. Together with the data from *PVhlKO* mice, we conclude that the β cell phenotypes most likely arise from increased β cell Hif-1α activation and consequent engagement of the Hif-1α–dependent gene expression program.

The VHL/HIF pathway has many downstream targets, and therefore abnormal β cell function in β*VhlKO* and *PVhlKO* mice is likely to be due to a combination of effects. We demonstrate marked abnormalities in GSIS in *Vhl*-deficient islets but no alterations in either β cell proliferation or survival. The molecular mechanisms underlying this defect include reduced *Glut2* expression, which has been shown to be sufficient to perturb glucose homeostasis in mice and humans (27, 28), and attenuated *Gck* expression, which alone (10, 29) or in combination with additional β cell defects (30) causes β cell dysfunction. Our findings also suggest that increased *Glut1* expression compromises appropriate glucose handling by β cells and does not compensate for the marked reduction in Glut2 expression. The K_m for D-glucose of rodent Glut2 is 17 mmol/l, allowing a wide range of physiological blood glucose levels to be sensed by the β cell. GLUT1, however, has been shown to have a K_m for D-glucose of 2.3–2.6 mmol/l in humans and to confer a human β cell V_{max} of 3 mmol/l/min, compared with a rodent β cell V_{max} of 32 mmol/l/min for glucose uptake via Glut2. This suggests that β*VhlKO* and *PVhlKO* islets relying on Glut1 to supply glucose into the β cell sense little difference between 2 and 20 mmol/l glucose, since Glut1 facilitates glucose transport at near maximum capacity at these concentrations. The absolute levels of glucose uptake depend on the absolute Glut1 expression levels, but our data show the increased Glut1 expression does not normalize glucose uptake in an appropriate manner to restore GSIS in *Vhl*-null islets.

We also demonstrate alterations in the expression of glycolytic genes that have an additional negative impact upon GSIS. Increased *Pdk1* expression inhibits pyruvate dehydrogenase activity and would restrict the entry of pyruvate to mitochondrial oxidative pathways, while reduced aldolase expression would be anticipated to reduce flux through glycolysis as well. Our studies using non-glucose secretagogues together with metabolic and imaging studies place the defects in GSIS proximal to the mitochondria. The combination of markedly reduced glucose uptake and impaired glycolytic flux would prevent the burst of mitochondrial oxidative phosphorylation required for quantitative coupling of glucose uptake to insulin release when glucose levels rise. Taken together, this combination provides a sufficient explanation for the abnormalities in β*VhlKO* and *PVhlKO* mice.

Recently it was reported that mice with β cell–specific deletion of the Hif-1α dimerization component *Arnt/Hif1b* show impaired glucose homeostasis (9). In contrast, our genetic manipulation of deleting *Vhl* in insulin-producing cells led to increased β cell Hif activity. While it might have been predicted that these 2 distinct perturbations of the Hif pathways would have opposite effects

upon glucose homeostasis, a number of explanations could underlie the similar phenotypes resulting from deletion of *Vhl* or *Arnt* in mouse β cells. Firstly, in addition to HIFα subunits, ARNT dimerizes with the aryl hydrocarbon receptor, and loss of the AHR/ARNT response may influence β cell function. Indeed, siRNA for *Ahr* was reported to decrease GSIS in the Min6 β cell line (9). Secondly, *Arnt* will have been deleted not only in β cells, but also in the hypothalamus, which could contribute to the reported abnormalities in glucose homeostasis seen in mice generated using the *RIPCre* animal (9). Third, glucose intolerance has been demonstrated in the pure *RIPCre* strain on certain genetic backgrounds, and our own use of *PdxCre* animals (14) provides evidence that the effect we observed was not due to the *RIPCre* transgene. We also demonstrate normal glucose tolerance in the *RIPCre* strain in our hands. Our studies of mice lacking *Hif1a* in insulin-producing cells give further insights into the role of this pathway in β cells and suggest that Hif-1α may have a mild restraining role on β cell function under basal conditions. There are additional considerations in evaluating the potential pathological relevance of our findings compared with those of Gunton et al. (9), which suggested that decreased HIF could contribute to human type 2 diabetes. First, type 2 diabetes is clearly multifactorial, and it is plausible that perturbations of HIF in either direction could contribute to its pathophysiology, although our studies with *Hif1a* deletion in β cells suggest that this may not be the case. Second, HIF activation by tissue hypoxia is a well-understood pathophysiological construct, whereas the circumstances under which HIF would be suppressed — other than by genetic manipulation — are unclear. In this context it is also important to appreciate that HIF is activated, at least in the kidney, in response to very minor alterations in oxygen delivery that are within the physiological range. Finally, our results indicate that although engagement of the HIF-1α–dependent transcriptional program would be anticipated to protect β cells from hypoxia, the consequence is perturbation of the intimate relationship between oxidative phosphorylation and GSIS, highlighting the complexity of the role of the VHL/HIF pathway in β cell function.

Our findings are likely to have clinical relevance independent of the putative role of the VHL/HIF pathway in human type 2 diabetes. Tissue oxygen delivery is reduced in many settings, including sepsis syndrome, acute and chronic pulmonary conditions, and obstructive sleep apnea. Indeed, sepsis and obstructive sleep apnea are associated with impaired glucose metabolism, and acute hypoxia causes glucose intolerance in humans (31). Our findings suggest that HIF activation in the β cell in these settings would impair GSIS. However, understanding the overall effects of the VHL/HIF pathway and hypoxia on metabolic networks in these human illnesses represents a complex challenge in systems biology, as it is unclear precisely which tissues may contribute to abnormal glucose handling in the setting of hypoxia in humans. However, a particular clinical scenario in which islet hypoxia may be relevant is islet transplantation. This potentially attractive therapy for diabetes is hampered by hypoxic graft failure, and it has been suggested that impaired graft function may occur in part through activation of the HIF pathway (32). Our studies show that this is likely and provide mechanisms by which this would occur. Our genetic experiments also suggest that pharmacological manipulation of the HIF system, which is under investigation as a therapeutic strategy in cancer, anemia, cardiac ischemia and failure (33), and inflammatory conditions such as glomerulonephritis (34), may have profound effects on β cell function unless this treatment is targeted to specific organs. *Vhl* is a tumor suppressor gene, and pancreatic cysts and tumors are a feature of human VHL disease (35). However, the β*VhlKO* and *PVhlKO* mice in our studies did not develop these types of tumors, although they did show some increase in vascularization. One explanation would be that the human tumors and cysts do not arise from β cells or other cells expressing *Pdx1*, which would reinforce the cell and tissue specificity of the tumor suppressor action of *Vhl*. An alternative possibility is that further events are required for the development of cysts and tumors in the pancreas, which typically present in the third and fourth decades in humans. An important question has been the extent of redundancy in the VHL/HIF system, and whether differential redundancy of HIF components between cell types might account for this striking tissue specificity of tumors in VHL disease (36). Our results may help to clarify this by showing that in β cells *Vhl* loss is sufficient for Hif-1α stabilization and activation, does not result in detectable Hif-2α activation, and does not produce an increase in β cell mass. The lack of Hif-2α activation is likely to reflect cell-type specificity in *Hif2a* mRNA expression and is consistent with a previous study in which acute hypoxia did not activate Hif-2α in rat islets (37). Interestingly in kidney cells, the site of malignant tumors in VHL patients, acquisition of *Hif2a* expression appears to be crucial in progression and tumor growth (15). Finally, it is becoming increasingly clear that the VHL/HIF pathway also has important physiological roles that may not necessarily be manifest as disease processes, such as involvement in innate immunity (5), in muscle performance (7), in neutrophil survival decisions (6), in stem cell differentiation and homing (38–40), and in the role of skin oxygen sensing (8).

In summary, our studies show that VHL/HIF oxygen-sensing mechanisms play a critical role in glucose homeostasis, and activation of this pathway causes β cell dysfunction.

Methods

Mice and animal care. Floxed *Vhl* allele (*Vhl*[+fl]; The Jackson Laboratory) mice were crossed with *RIPCre* mice (The Jackson Laboratory) and *PdxCre* mice (14) to generate compound heterozygote mice for both Cre strains. Double heterozygote mice were crossed with *Vhl*[+fl] mice to obtain WT, *Vhl*^{fl/fl}, *Cre*, and *Cre Vhl*^{fl/fl} mice for each Cre strain. Mice lacking *Vhl* in *RIPCre*-expressing cells were designated β*VhlKO* mice, and those lacking *Vhl* in *PdxCre*-expressing cells were designated *PVhlKO* mice. *Hif1a*[+fl] mice (41) were intercrossed with *RIPCre* mice and compound heterozygote mice mated with *Hif1a*[+fl] mice to obtain mice lacking *Hif1a* in insulin-producing cells, designated β*Hif1aKO* mice. β*Hif1aKO* mice were intercrossed with *RIPCre Vhl*^{fl/fl}, and compound heterozygote mice for all alleles were subsequently crossed to generate mice lacking both *Vhl* and *Hif1a* in insulin-producing cells, designated β*VhlHif1aKO* mice. Mice were maintained on a 12-hour light/12-hour dark cycle with free access to water and standard mouse chow (4% fat, RM1; Special Diet Services) and housed in specific pathogen–free barrier facilities. Mice handling and all in vivo studies were performed in accordance with the United Kingdom Home Office Animal Procedures Act of 1986 and with approval of the University College London Animal Ethics Committee. All mice were studied on a mixed 129S/C57BL/6 background with appropriate littermate controls. WT, *Cre* transgenic, and *Vhl*^{fl/fl} mice were phenotypically indistinguishable with no differences in glucose tolerance between WT, *Cre* transgenic, and *Vhl*^{fl/fl} mice for both β*VhlKO* and *PVhlKO* strains (Supplemental Figure 5, C and D). Balanced numbers of mice of these genotypes were therefore used as controls. All phenotypes described for the mice in Results were present in both male and female animals. Genotyping of the mice was performed by PCR amplification of tail DNA as previously described (11, 12, 14). Cre-mediated excision of *Vhl* was detected

by PCR on genomic DNA isolated from pancreatic islets and hypothalami. DNA (150 ng) was assayed on the Opticon 2 system (MJ Research) using the primers mVHLPCR5 (5′-CAAACTGCATGCCTGGTACCCAC-3′) and mVHLPCR8 (5′-CTGACTTCCACTGATGCTTGTCACAG-3′).

Physiological measurements. Body and tissue weights were determined using a Sartorius BP610 balance. Blood samples were collected from mice via tail vein bleeds or from cardiac puncture on terminally anesthetized mice. Blood glucose was measured using an Ascensia Elite Glucometer (Bayer Corp.). Plasma insulin levels were determined using an ultrasensitive rat insulin ELISA (Crystalchem Inc.) using a mouse standard or with a mouse ELISA (Linco Research). Glucose tolerance tests and GSIS tests were performed on mice after a 16-hour fast as previously described (14). Animals were injected intraperitoneally with 2 g/kg or 3 g/kg D-glucose, and blood glucose or insulin levels, respectively, were determined.

Immunohistochemistry and morphometric analysis. Immunohistochemistry for insulin and glucagon and morphometric analysis were performed using methods described previously (12, 14). Antibodies used were as follows: mouse anti-insulin antibody (clone K36aC10; Sigma-Aldrich), rabbit anti-glucagon antibody (Abcam), chicken anti-mouse IgG–Alexa Fluor 488 conjugate, and anti-rabbit IgG–Alexa Fluor 594 (Invitrogen). For immunostaining of Hif-1α (rabbit polyclonal; Novus Inc.), Glut1 (rabbit polyclonal; Alpha Diagnostics Ltd.), Cd31 (rabbit polyclonal; Santa Cruz Biotechnology Inc.), and Glut2 (rabbit polyclonal, gift from B. Thorens, University of Lausanne, Lausanne, Switzerland) in paraffin-embedded sections, antigen retrieval with DAKO target retrieval was performed, and for visualization either a DAKO CSA kit or DAKO Envision kit or anti-rabbit Alexa Fluor 594–conjugated secondary antibodies were used according to the manufacturers' instructions. For Hif-1α and insulin double-staining, paraffin-embedded sections were first immunostained and visualized for Hif-1α (rabbit polyclonal, Alpha Diagnostics) using the DAKO CSA kit. After visualization, sections were immunostained with mouse anti-insulin antibody (clone K36aC10; Sigma-Aldrich) and Alexa Fluor 488–conjugated chicken anti-mouse IgG. Mounting solution containing DAPI (VECTASHIELD DAPI; Vector Laboratories) was used to identify nuclei. For detection of apoptosis, rabbit anti–active caspase-3 antibody (BD Biosciences — Pharmingen) was used, and to detect proliferation, rabbit anti-Ki67 antibody (Abcam) was used, both as previously described (14). Sections were imaged via light, fluorescence, or confocal microscopy, and images were captured as previously described (12, 14).

Western blotting. Urea-SDS lysis buffer was used to prepare protein lysates, and protein concentrations were measured using BCA (Pierce Biotechnology). Lysates were run on SDS/PAGE gels and then transferred to Immobilon-P PVDF membranes (Millipore). Membranes were blocked in 5% milk/1% BSA for 45 minutes and primary antibodies applied for 2 hours at room temperature. Membranes were then washed and incubated with an HRP-linked secondary antibody (DAKO) for 1 hour at room temperature. Following further washes, the membrane was developed with ECL plus (Amersham Biosciences). Primary antibodies used were Hif-1α, Glut1, and Glut2 as described above, and α-tubulin (Sigma-Aldrich).

Islet and Min6 cell experiments. Mice were sacrificed by cervical dislocation, and the common bile duct was cannulated and its duodenal end occluded by clamping. Liberase solution (2 ml at 0.25 mg/ml in HBSS) was injected into the duct to distend the pancreas. The pancreas was excised, incubated at 37°C for 15 minutes, and mechanically disrupted in 10 ml of HBSS (supplemented with 1% BSA). Cellular components were collected by centrifugation (201 g for 1 minute), washed, and resuspended in 10 ml of HBSS. Islets were hand-picked under a microscope and washed once in HBSS. Prior to DNA or protein extraction, islets were collected by centrifugation at 5,724 g for 2 minutes and stored at –80°C. For insulin secretion studies, isolated islets were cultured overnight in DMEM with 11 mmol/l glucose. Medium was replaced with KRBH (Krebs-Ringer buffer containing 2 mmol/l D-glu-cose and 10 mmol/l HEPES) 1 hour prior to study. Dynamic insulin release was then assessed using a multichamber perifusion system at 37°C in a temperature-controlled environment, as previously described (42). Insulin was measured in perifusate samples by radioimmunoassay, as previously described (42). Static insulin release was assessed using batch cultures of 5 islets in 150 μl KRBH plus additional D-glucose, 25 mmol/l KCl, or 10 mmol/l α-ketoisocaproic acid (Sigma-Aldrich) for 1 hour at 37°C. Insulin release was measured by ELISA. Min6 cells were cultured as previously described (42). To activate Hif-1α, cells were incubated in 1% oxygen or 0.5 mmol/l dimethyloxalylglycine for 16 hours. For examination of gene expression in Min6 cells, retroviral transduction with active HIF-1α (P402A and P564A) was performed as previously described (19). GSIS from infected Min6 cells was measured by static culture in a 96-well plate (3 × 10^4 cells per well). Following overnight culture, media was replaced with KRBH for 1 hour before static secretion assays were performed (as described above).

Gene expression studies. Isolated islets or Min6 cells were harvested and RNA extracted immediately with RNABee reagent (Biogenesis) or RNeasy kits (Qiagen) according to the manufacturers' instructions. Total RNA (0.5–2 μg) was reverse transcribed using a first-strand cDNA synthesis kit (Roche). Quantitative PCR was carried out with first-strand cDNA and commercial TaqMan Assays (Applied Biosystems) on the Opticon 2 System (MJ Research Inc.). Expression levels of *Glut1*, *Glut2*, *Gck*, *Ecad*, *Nkx6.1*, *NeuroD1*, *Hnf3b*, *Hnf1a*, *Hnf4a*, *Pfk*, *Aldolase*, *Gapdh*, *Pdk1*, *Vhl*, and *Cd31* were normalized to hypoxanthine-guanine phosphoribosyl transferase (*Hprt*), and data were analyzed using the $2^{-\Delta\Delta CT}$ method (12). Details of the primers used are presented in Supplemental Methods.

Imaging studies in isolated islets. Islets isolated as described above were dissociated into single cells by incubation in trypsin at 21°C for 2.5 min with gentle agitation. Cells were washed once before being allowed to attach to poly-L-lysine–treated glass coverslips. Cells were incubated for 48 hours in DMEM culture medium with L-glutamine supplemented with 10% heat-inactivated FBS and 5.5 mmol/l D-glucose. The medium was changed to HBSS supplemented with 20 mmol/l HEPES and 2 mmol/l D-glucose 1 hour prior to imaging. Cells were imaged on a 37°C heated stage on a Zeiss LSM 510 confocal microscope. β cells were stained following analysis, using dithizone for identification (43). Uptake of the fluorescent glucose analogue 2-NBDG (Invitrogen) was measured by addition of 18 nmol/l 2-NBDG in the presence of 2.5 mmol/l D-glucose during continuous imaging with an excitation wavelength of 458 nm and collection of light emitted at greater than 505 nm (20). Reduced NADH and oxidized flavoprotein (FAD^{++}) autofluorescence in response to the addition of D-glucose in 9 mmol/l increments were captured as previously described (21, 44). The mitochondrial uncoupler carbonyl cyanide p-trifluoromethoxyphenylhydrazone (FCCP) was used to artificially evoke maximally oxidized states of the NADH/flavoproteins to establish the dynamic range of the signals. Ca^{2+} imaging using Fura-2AM was performed as previously described (21, 44). Measurements were obtained by averaging the signal collected in a region of interest drawn across the maximum area of the β cell. Mono-methyl succinate (Fluka) and tolbutamide (Sigma-Aldrich) were used to stimulate Ca^{2+} influx via mitochondrial metabolism and pharmacological K$_{ATP}$ channel closure respectively.

Statistics. Data are presented as mean ± SEM, unless otherwise indicated. All statistics were performed using Minitab (version 13) and GraphPad (Prism 4) software. Paired and unpaired t tests and 1- and 2-way ANOVA were performed, using the post-hoc Newman-Keuls test where appropriate. $P < 0.05$ was regarded as statistically significant.

Acknowledgments

Address correspondence to: Dominic J. Withers, Centre for Diabetes and Endocrinology, University College London, Rayne Institute, 5 University Street, London WC1E 6JJ, United Kingdom. Phone: 00442076796586; Fax: 00442076796583; E-mail: d.withers@ucl.ac.uk. Or to: Patrick H. Maxwell, Centre for Cell Signalling and Molecular Genetics, University College London, Rayne Institute, 5 University Street, London WC1E 6JJ, United Kingdom. Phone: 00442076796351; Fax: 00442076796211; E-mail: p.maxwell@ucl.ac.uk.

James Cantley's present address is: Diabetes and Obesity Research Program, Garvan Institute of Medical Research, Sydney, New South Wales, Australia.

Colin Selman's present address is: Institute of Biological and Environmental Sciences, University of Aberdeen, Aberdeen, United Kingdom.

1. Schuit, F.C., Huypens, P., Heimberg, H., and Pipeleers, D.G. 2001. Glucose sensing in pancreatic beta-cells: a model for the study of other glucose-regulated cells in gut, pancreas, and hypothalamus. *Diabetes.* **50**:1–11.
2. Semenza, G.L. 1999. Regulation of mammalian O2 homeostasis by hypoxia-inducible factor 1. *Annu. Rev. Cell Dev. Biol.* **15**:551–578.
3. Maxwell, P.H., et al. 1999. The tumour suppressor protein VHL targets hypoxia-inducible factors for oxygen-dependent proteolysis. *Nature.* **399**:271–275.
4. Kaelin, W.G. 2005. Proline hydroxylation and gene expression. *Annu. Rev. Biochem.* **74**:115–128.
5. Rius, J., et al. 2008. NF-kappaB links innate immunity to the hypoxic response through transcriptional regulation of HIF-1alpha. *Nature.* **453**:807–811.
6. Walmsley, S.R., et al. 2005. Hypoxia-induced neutrophil survival is mediated by HIF-1alpha-dependent NF-kappaB activity. *J. Exp. Med.* **201**:105–115.
7. Mason, S.D., et al. 2004. Loss of skeletal muscle HIF-1alpha results in altered exercise endurance. *PLoS Biol.* **2**:e288.
8. Boutin, A.T., et al. 2008. Epidermal sensing of oxygen is essential for systemic hypoxic response. *Cell.* **133**:223–234.
9. Gunton, J.E., et al. 2005. Loss of ARNT/HIF1beta mediates altered gene expression and pancreatic-islet dysfunction in human type 2 diabetes. *Cell.* **122**:337–349.
10. Postic, C., et al. 1999. Dual roles for glucokinase in glucose homeostasis as determined by liver and pancreatic beta cell-specific gene knock-outs using Cre recombinase. *J. Biol. Chem.* **274**:305–315.
11. Haase, V.H., Glickman, J.N., Socolovsky, M., and Jaenisch, R. 2001. Vascular tumors in livers with targeted inactivation of the von Hippel-Lindau tumor suppressor. *Proc. Natl. Acad. Sci. U. S. A.* **98**:1583–1588.
12. Choudhury, A.I., et al. 2005. The role of insulin receptor substrate 2 in hypothalamic and beta cell function. *J. Clin. Invest.* **115**:940–950.
13. Herrera, P.L. 2000. Adult insulin- and glucagon-producing cells differentiate from two independent cell lineages. *Development.* **127**:2317–2322.
14. Cantley, J., et al. 2007. Pancreatic deletion of insulin receptor substrate 2 reduces beta and alpha cell mass and impairs glucose homeostasis in mice. *Diabetologia.* **50**:1248–1256.
15. Raval, R.R., et al. 2005. Contrasting properties of hypoxia-inducible factor 1 (HIF-1) and HIF-2 in von Hippel-Lindau-associated renal cell carcinoma. *Mol. Cell. Biol.* **25**:5675–5686.

16. Jaakkola, P., et al. 2001. Targeting of HIF-alpha to the von Hippel-Lindau ubiquitylation complex by O2-regulated prolyl hydroxylation. *Science.* **292**:468–472.
17. Sander, M., et al. 2000. Homeobox gene Nkx6.1 lies downstream of Nkx2.2 in the major pathway of beta-cell formation in the pancreas. *Development.* **127**:5533–5540.
18. Yamagata, K., et al. 2002. Overexpression of dominant-negative mutant hepatocyte nuclear factor-1 alpha in pancreatic beta-cells causes abnormal islet architecture with decreased expression of E-cadherin, reduced beta-cell proliferation, and diabetes. *Diabetes.* **51**:114–123.
19. Esteban, M.A., et al. 2006. Regulation of E-cadherin expression by VHL and hypoxia-inducible factor. *Cancer Res.* **66**:3567–3575.
20. Yamada, K., et al. 2000. Measurement of glucose uptake and intracellular calcium concentration in single, living pancreatic beta-cells. *J. Biol. Chem.* **275**:22278–22283.
21. Duchen, M.R., Surin, A., and Jacobson, J. 2003. Imaging mitochondrial function in intact cells. *Methods Enzymol.* **361**:353–389.
22. Carlsson, P.O., Liss, P., Andersson, A., and Jansson, L. 1998. Measurements of oxygen tension in native and transplanted rat pancreatic islets. *Diabetes.* **47**:1027–1032.
23. Frew, I.J., and Krek, W. 2008. pVHL: a multipurpose adaptor protein. *Sci. Signal.* **1**:pe30.
24. Okuda, H., et al. 2001. The von Hippel-Lindau tumor suppressor protein mediates ubiquitination of activated atypical protein kinase C. *J. Biol. Chem.* **276**:43611–43617.
25. Iturrioz, X., et al. 2006. The von Hippel-Lindau tumour-suppressor protein interaction with protein kinase Cdelta. *Biochem. J.* **397**:109–120.
26. Mukhopadhyay, D., Knebelmann, B., Cohen, H.T., Ananth, S., and Sukhatme, V.P. 1997. The von Hippel-Lindau tumor suppressor gene product interacts with Sp1 to repress vascular endothelial growth factor promoter activity. *Mol. Cell. Biol.* **17**:5629–5639.
27. Santer, R., et al. 1997. Mutations in GLUT2, the gene for the liver-type glucose transporter, in patients with Fanconi-Bickel syndrome. *Nat. Genet.* **17**:324–326.
28. Ohtsubo, K., et al. 2005. Dietary and genetic control of glucose transporter 2 glycosylation promotes insulin secretion in suppressing diabetes. *Cell.* **123**:1307–1321.
29. Bell, G.I., and Polonsky, K.S. 2001. Diabetes mellitus and genetically programmed defects in beta-cell

function. *Nature.* **414**:788–791.
30. Terauchi, Y., et al. 1997. Development of non-insulin-dependent diabetes mellitus in the double knockout mice with disruption of insulin receptor substrate-1 and beta cell glucokinase genes. Genetic reconstitution of diabetes as a polygenic disease. *J. Clin. Invest.* **99**:861–866.
31. Oltmanns, K.M., et al. 2004. Hypoxia causes glucose intolerance in humans. *Am. J. Respir. Crit. Care Med.* **169**:1231–1237.
32. Moritz, W., et al. 2002. Apoptosis in hypoxic human pancreatic islets correlates with HIF-1alpha expression. *FASEB J.* **16**:745–747.
33. Sano, M., et al. 2007. p53-induced inhibition of Hif-1 causes cardiac dysfunction during pressure overload. *Nature.* **446**:444–448.
34. Ding, M., et al. 2006. Loss of the tumor suppressor Vhlh leads to upregulation of Cxcr4 and rapidly progressive glomerulonephritis in mice. *Nat. Med.* **12**:1081–1087.
35. Kaelin, W.G., Jr., and Maher, E.R. 1998. The VHL tumour-suppressor gene paradigm. *Trends Genet.* **14**:423–426.
36. Maxwell, P.H. 2004. HIF-1's relationship to oxygen: simple yet sophisticated. *Cell Cycle.* **3**:156–159.
37. Wiesener, M.S., et al. 2003. Widespread hypoxia-inducible expression of HIF-2alpha in distinct cell populations of different organs. *FASEB J.* **17**:271–273.
38. Covello, K.L., et al. 2006. HIF-2alpha regulates Oct-4: effects of hypoxia on stem cell function, embryonic development, and tumor growth. *Genes Dev.* **20**:557–570.
39. Gustafsson, M.V., et al. 2005. Hypoxia requires notch signaling to maintain the undifferentiated cell state. *Dev. Cell.* **9**:617–628.
40. Ceradini, D.J., et al. 2004. Progenitor cell trafficking is regulated by hypoxic gradients through HIF-1 induction of SDF-1. *Nat. Med.* **10**:858–864.
41. Schipani, E., et al. 2001. Hypoxia in cartilage: HIF-1alpha is essential for chondrocyte growth arrest and survival. *Genes Dev.* **15**:2865–2876.
42. Persaud, S.J., et al. 2002. A key role for beta-cell cytosolic phospholipase A(2) in the maintenance of insulin stores but not in the initiation of insulin secretion. *Diabetes.* **51**:98–104.
43. Shiroi, A., et al. 2002. Identification of insulin-producing cells derived from embryonic stem cells by zinc-chelating dithizone. *Stem Cells.* **20**:284–292.
44. Dumollard, R., et al. 2004. Sperm-triggered [Ca2+] oscillations and Ca2+ homeostasis in the mouse egg have an absolute requirement for mitochondrial ATP production. *Development.* **131**:3057–3067.